Catalysis Science and Technology

ARTICLE

Upgrading of diols by gas-phase dehydrogenation and dehydration reactions on bifunctional Cu-based oxides

P. A. Torresi, V.K. Díez, P.J. Luggren and J.I. Di Cosimo*,

Biomass-derived short chain polyols can be transformed in valuable oxygenates used as building blocks. The gas phase conversion of a model molecule of 1,3-diols (1,3-butanediol) was studied on bifunctional Cu-Mg, Cu-Al and Cu-Mg-Al mixed oxide catalysts that combine surface Cu^0 particles and acid-base properties. A series of ZCuMgAl catalysts (Z=0.3-61.2 wt.% Cu, Mg/Al=1.5 molar ratio) was prepared by coprecipitation and thoroughly characterized by several techniques such as BET surface area, TPR-N_2O chemisorption, XRD and TPD of CO_2. The ZCuMgAl catalysts promote the upgrading of the diol by a series of dehydrogenation and/or dehydration reactions proceeding at reaction rates that depend on the copper content (Z). The overall activity increases linearly with the amount of surface Cu^0 species thereby confirming participation of metallic sites in rate-limiting steps. Besides, surface Cu^0 sites favor the reaction pathway toward 1,3-butanediol dehydrogenation. Thus, the dehydrogenation/dehydration selectivity ratio increases with Z as a result of the enhanced amount of exposed Cu^0 particles. ZCuMgAl catalysts with Z < 8wt.% dehydrogenate-dehydrate-hydrogenate the diol at low rates giving mainly C_4 ketones and break the intermediates forming C_1-C_3 oxygenates; catalysts with Z > 8wt.% are more active and yield valuable multifunctional C_4 oxygenates such as hydroxyketones and to a lesser extent, unsaturated alcohols and ketones. A strongly basic Cu-Mg catalyst promotes the C-C bond cleavage reaction giving short carbon chain oxygenates at low rates; an acidic Cu-Al catalyst converts the diol into the C_4 saturated ketone and olefins.

1. Introduction

Molecules containing multiple OH groups (polyols) present potential applications as organic building blocks. In the last decade it has been demonstrated that C_2-C_4 polyols such as glycerol, ethane-, propane- and butanediols can be obtained from biomass resources.[1,2] All these molecules can be used to produce hydrocarbon fuels by cracking reactions[3] or hydrogen via reforming processes.[4] Furthermore, transformation of all of the OH groups or of one in particular, can lead to other value-added oxygenates or chemicals used in organic synthesis.

Many strategies have been postulated to convert polyols into valuable oxygenates such as unsaturated alcohols,[5,6] furans,[7] hydroxycarbonyl compounds[8,9,10,11] and unsaturated carbonyl compounds,[6,12] as well as into olefins[6] and other products. Reactions like dehydration, dehydration coupled with hydrogen transfer, dehydrogenation, oxidation, hydrogenolysis or tandem dehydrogenation-dehydration-hydrogenation can be used for these purposes. Some of these strategies require the supply of H_2, water or other molecules to the reaction system.

Butanediols can be synthesized from renewable feedstocks such as glycerol and bioethanol by fermentation[13] or catalytic[14,15] routes. In particular, 1,3-butanediol (1,3-BDO), is a C_4 diol that can be considered as a model molecule for the catalytic upgrade of polyols because it contains one primary and one secondary hydroxyl function.

The strategy considered here is the gas phase valorization of the model 1,3-BDO molecule without reactant dilution in water and without supply of costly H_2. Thus, we postulate the conversion of 1,3-BDO by dehydrogenation and dehydration reactions that give rise to a variety of valuable compounds, grouped under different codes in Scheme 1. Initial dehydrogenation of just one OH group of 1,3-BDO leads to aldol compounds (hydroxyketone and hydroxyaldehyde of group HY). These molecules combining OH and C=O functions in aldol units are present in many pharmaceutical and food formulations and in organic synthesis intermediates.[16,17,18] On the other hand, initial 1,3-BDO dehydration yields unsaturated alcohols (group UOL) which are used in polymer industry. After initial 1,3-BDO dehydration or dehydrogenation reactions, consecutive dehydration, hydrogenation or isomerization reactions yield saturated and unsaturated ketones (group K) and saturated alcohols (group SOL) which are important intermediates for the

*Catalysis Science and Engineering Research Group (GICIC), INCAPE, UNL-CONICET. Santiago del Estero 2654. (3000) Santa Fe, Argentina.
Prof. J. Isabel Di Cosimo. Email: dicosimo@fiq.unl.edu.ar; TE:54-342-4511546, Ext 1558; FAX: 54-342- 4511170
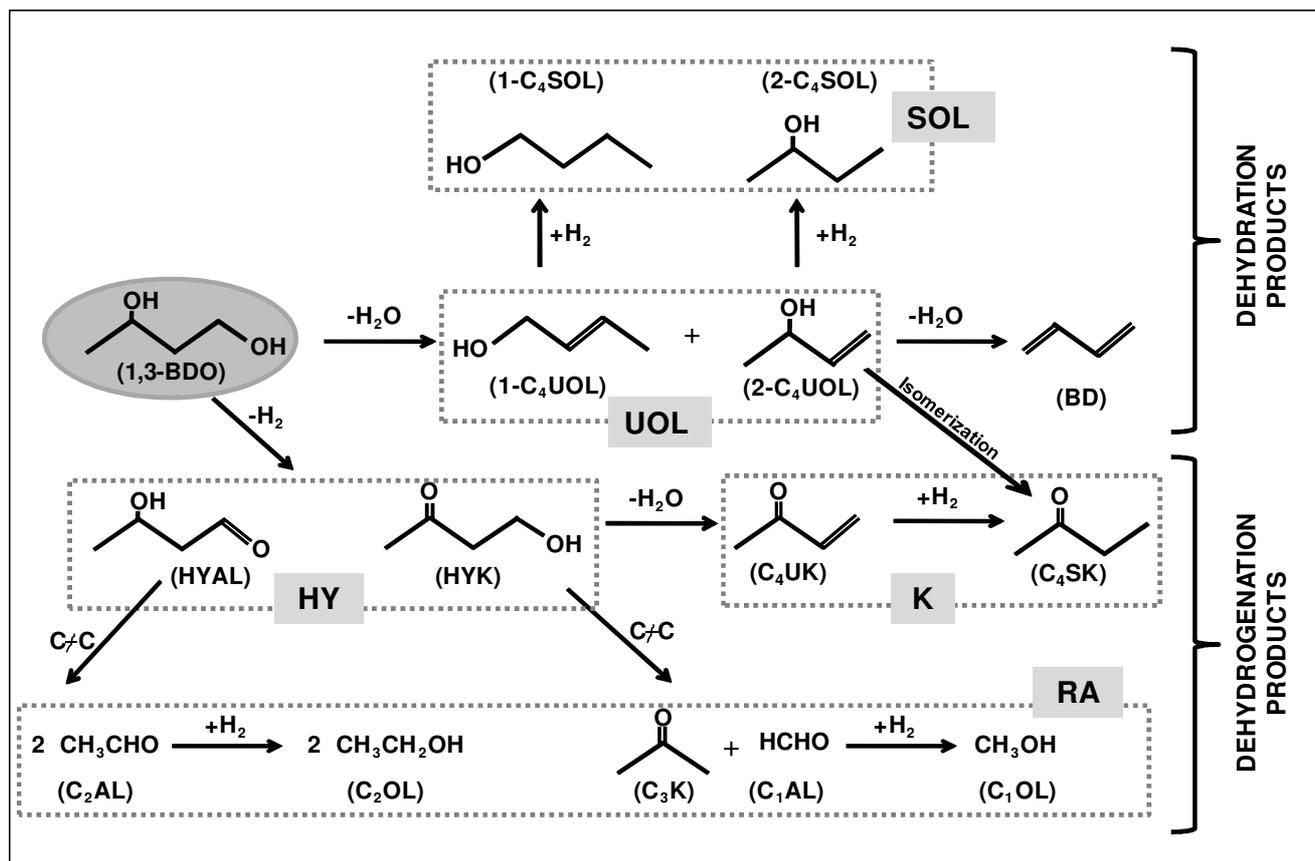
Scheme 1: Main reaction pathways for gas-phase 1,3-butanediol conversion.

synthesis of solvents, pesticides, terpenoids, as well as steroids, anticancer and other medical drugs.[19]

In previous works we investigated the conversion of 1,3-BDO on Cu/SiO_2 catalysts[20] and on acid-base single oxides with different electronegativities.[21] We demonstrated that Cu^0 sites in Cu/SiO_2 catalysts promote not only dehydrogenation but also dehydration steps at high rates. Main products fluctuate between the saturated ketone (in group K) and the hydroxyketone (in group HY) depending on the Cu^0 particle size. Unsaturated oxygenates (groups UOL and K) cannot be synthesized on these catalysts. On acid-base oxides the activity decreases 200-fold compared to Cu/SiO_2, and neither the saturated ketone nor the hydroxyketone are obtained, regardless of the oxide electronegativity. However, the product distribution on acid-base single oxides can be tuned to other dehydrogenation or dehydration products by increasing the oxide electronegativity. Therefore, the unsaturated ketone (in group K) and the unsaturated alcohols (group UOL) are obtained on low-electronegativity oxides whereas group UOL and olefins are mainly formed on more electronegative oxides. In conclusion, the activity and selectivity for 1,3-BDO conversion noticeably depend on the presence or not of a metallic function in the catalyst formulation and on the catalyst acid-base properties.

In this work we continue our studies on the gas-phase conversion of 1,3-BDO. We report the catalytic results obtained with Cu-Mg-Al mixed oxides that combine a metallic function provided by copper with mild acid-base properties. We base our research on the fact that many industrial processes involving synthesis or transformation of alcohols use copper in contents of up to 70 atom%.[22] Besides, we have shown that conversion of alcohols, such

as 2-propanol, proceeds at high rates on catalysts that contain a metallic function (Cu^0) in addition to an acid or base site provided by a single oxide.[23] Thus, the purpose of the present work is to investigate the feasibility of using a bifunctional metal/acid-base catalyst for conversion of 1,3-BDO toward value-added oxygenates. Specifically, we address our research to explore if a Cu-Mg-Al combination in the catalyst formulation enables formation of multifunctional chemical compounds such as those containing C=O and OH (group HY) or C=C and C=O (unsaturated ketone in group K) or C=C and OH (group UOL). With this purpose, a series of copper containing ZCuMgAl catalysts (Z = 0.3-61.2 wt.% Cu, Mg/Al = 1.5 molar ratio) was prepared, thoroughly characterized by several techniques and tested in the 1,3-BDO conversion. We found that 1,3-BDO is transformed on ZCuMgAl catalysts by similar reactions as those previously discussed for Cu/SiO_2 and acid-base single oxides[20,21] but with a different activity and selectivity. The role of the size and amount of exposed Cu^0 particles on the reactant conversion rate was investigated. Furthermore, we elucidated the participation of the catalyst surface acid-base or metal site in determining the initial dehydration or dehydrogenation pathway.

2. Experimental

2.1 Catalyst synthesis

Cu-based catalysts containing 0.3-61.2wt.% Cu were prepared by co-precipitation. Catalyst precursors of ternary Cu-Mg-Al mixed oxides were prepared by co-precipitation at a constant pH of 10.[23] After filtering, washing and drying at 363K, the precipitates

were decomposed overnight in air at 773K in order to obtain the corresponding mixed oxides with a Mg/Al = 1.5 molar ratio. These catalysts were denoted ZCuMgAl, where Z is the copper content expressed in wt.%. Following similar procedures binary 9.8CuMg and 6.4CuAl catalysts were prepared.

High-surface area magnesium oxide was prepared by hydration with distilled water of low-surface area commercial MgO (Carlo Erba 99%; 27m^2/g) and further decomposition of the resulting Mg(OH)$_2$ in a N$_2$ flow for 18 h at 773K.[24] Alumina was a commercial sample of γ-Al$_2$O$_3$ Cyanamid Ketjen CK 300.

2.2 Catalyst characterization

BET surface areas (*SA*) were measured by N$_2$ physisorption at its boiling point using an Autosorb Quantachrome 1-C sorptometer. The sample structural properties were determined by X-Ray Diffraction (XRD) technique using a Shimadzu XD-D1 instrument. The chemical content (Z) of Cu in all Cu-based catalysts was analyzed by Atomic Absorption Spectrometry (AAS).

Catalyst base site numbers (n_b) were measured by temperature-programmed desorption (TPD) of CO$_2$ preadsorbed at room temperature. Samples were exposed to a flowing mixture of 3% of CO$_2$ in N$_2$ until surface saturation. Weakly adsorbed CO$_2$ was removed by flushing with N$_2$. Finally, the temperature was increased to 773K at a ramp rate of 10K/min. The desorbed CO$_2$ was converted into CH$_4$ on a Ni/Kieselghur catalyst at 673K and then analyzed using a flame ionization detector (FID).[23]

The dispersion of the metallic copper particles (*D*), defined as the ratio of the number of surface metallic copper atoms (Cu^S) to the total copper atoms in the catalyst formulation measured by AAS (Cu^T_{AAS}). *D* values were determined by two consecutive experiments of temperature programmed reduction (TPR), using a reducing mixture of 5 % H$_2$/Ar at a flow rate of 50 cm^3/min and loading the reactor with the same molar amount of copper (150μmol) in each experiment.[20] Conditions were chosen following the criteria of Monti et al.[25] and Malet et al.[26] Heating rates of 10 K/min from 298 to typically 623 K were used. A mass spectrometer (MS) in a Baltzers Omnistar unit monitored the hydrogen consumption. Quantitative H$_2$-uptakes were calculated by integration of the two experimental TPR curves and using previous calibration with CuO powder (Cicarelli, PA). Thus, from the first TPR experiment, Cu^T_{TPR} values were obtained, representing the total amount of reducible copper species up to 623 K. The second TPR experiment was carried out after re-oxidation of the surface copper metal atoms to Cu$_2$O using N$_2$O and a stoichiometry of Cu^S/N$_2$O = 2.[27] The sample degree of reduction was defined as $Cu^T_{TPR}/Cu^T_{AAS} \times 100$. Assuming a Cu surface density of 1.47×10^{19} Cu atoms/m^2 and spherical Cu crystallites,[28] the Cu^0 specific surface area was calculated as A_{Cu} (m^2/g cat) = $6.44\ D \times Z$ and the average copper particle size was determined as L (nm) = 1.04/D.

2.3 Catalytic testing

Vapor-phase conversion of 1,3-butanediol (1,3-BDO) was carried out at 493-533K and 101.3 kPa in a fixed-bed reactor at contact times (W/F^0_{BDO}) of 0.5-33.0 g cat h/mol of 1,3-butanediol. Before the catalytic tests, catalysts were pretreated in a flow of N$_2$ at 773K for 1 h. Then, the Cu-containing catalysts were reduced in situ in flowing H$_2$ (35 cm^3/min) at 573 K for 1 h. 1,3-BDO (Aldrich GC, 99.0%) was introduced via a syringe pump and vaporized into flowing N$_2$ (150 cm^3/min) to give a 1,3-BDO partial pressure ($\bar{P}_{BDO}$) of 2.3 kPa. Reaction products were analyzed by on-line gas chromatography using an Agilent 7890A chromatograph equipped with flame ionization detector and a 0.2% Carbowax 1500/80-100 Carbopack C packed column. Data were collected every 0.5 h for 5

h. Main reaction products were identified as 4-hydroxy-2-butanone (HYK), 2-butanone (C$_4$SK), 3-buten-2-one (C$_4$UK), acetaldehyde (C$_2$AL), methanol (C$_1$OL), ethanol (C$_2$OL), acetone (C$_3$K), 3-buten-2-ol (2-C$_4$UOL), 2-buten-1-ol (1-C$_4$UOL), 2-butanol (2-C$_4$SOL), 1-butanol (1-C$_4$SOL) and butadiene (BD). Due to a slight catalyst deactivation process, the catalytic results reported here were calculated by extrapolation of the reactant and product concentration curves to zero time on stream. Then, X_{BDO}, and S represent conversion and selectivity at t=0, respectively. Turnover rates (TOR) are defined as the moles of reactant converted per mol of Cu^0 surface site and per second.

3. Results and Discussion

3.1. Characterization of ZCuMgAl mixed oxides

A set of bifunctional Cu-containing ZCuMgAl mixed oxides was prepared by coprecipitation and characterized by several techniques. Mg^{2+} and Al^{3+} were selected because of the known basic and acidic properties, respectively, of their corresponding single oxides.[21,29] All these oxides have a constant Mg/Al molar ratio of 1.5 but the copper content was varied between 0.3 and 61.2 wt%. We chose that Mg/Al ratio because similar materials, due to their mild basic properties, were successfully applied to conversion of other alcohols such as 2-propanol by dehydrogenation-aldol condensation reactions[30] and to reduction of unsaturated ketones toward unsaturated alcohols by hydrogen transfer.[31] On the other hand, 9.8CuMg and 6.4CuAl catalysts were prepared to represent typically, bifunctional metal-base or metal-acid catalysts, respectively. The physicochemical properties of the ZCuMgAl mixed oxides are presented in Table 1, as well as those of the reference materials.

Water and CO$_2$ removal during calcination generates a porous structure that is responsible for the high mixed oxide surface area (*SA*).[32] As can be seen in Table 1, the *SA* values are rather independent of the copper content for Z ≤ 15.1 wt.%. However, for Z > 15.1 wt.% the *SA* values are remarkably lower as a consequence of the decreased content of Al^{3+} cations. Aluminum is known to be a textural promoter in Mg-Al or Cu-Zn-Al catalysts,[32,33] and the low content of this metal gives rise to large CuO particles, as will be discussed below, that may block the oxide pores, thereby reducing the accessible *SA*.

The thermal decomposition of the coprecipitated Cu-Mg-Al catalyst precursors gives rise to poorly crystalline mixed oxides, Figure 1. The structural analysis and the identification of the crystalline phases present in the ZCuMgAl oxides were carried out by XRD. Figure 1 shows a single quasi-amorphous MgO (periclase, ASTM 4-0829) phase at low copper contents (Z<15.1 wt.%). No crystalline AlOx species was detected at any Z value, in agreement with previous work on Mg-Al mixed oxides showing that for Mg/Al molar ratios in the range of 1-9, the Al^{3+} cations remain closely associated with the MgO structure after calcination.[32] The incorporation of the Al^{3+} cations in the MgO matrix is evident in the diffractograms of Figure 1; the shift of the (200) diffraction line position (~43°) towards higher 2θ values compared to that of pure MgO (42.87°), is an indication of substitution of Al^{3+} for Mg^{2+} in the periclase structure. Calculations of the MgO lattice parameter (a_{MgO}), Table 1, show a contraction of the MgO unit cell in the ZCuMgAl oxides compared with that of pure MgO as a result of the incorporation of smaller Al^{3+} cations in the structure. These a_{MgO} values are in agreement with the 4.175 nm reported by Sato et al.[34] for a Mg-Al mixed oxide with a similar Mg/Al molar ratio. Although the Mg/Al ratio is constant in all the ZCuMgAl oxides, the a_{MgO} values decrease with increasing Z as will be discussed later.

Table 1: Physicochemical properties of ZCuMgAl, 9.8CuMg, 6.4CuAl, MgO and Al$_2$O$_3$ catalysts and TOR values for copper-based catalysts

Catalyst	Surface area, SA (m^2/g)	Nominal composition (wt.%)			Structural analysis by XRD		Cu species reducibility, dispersion and size				Basic properties	TOR^g (s^{-1})
		Cu	Mg	Al	$a_{MgO}{}^a$ (Å)	Phases detected	D^b (%)	$A_{Cu}{}^c$ (m^2/g)	L^d (nm)	$T_M{}^e$ (K)	$n_b{}^f$ (μmol/g)	
0.3CuMgAl	217	0.5	32.9	23.7	4.167	MgO	-	-	-	-	527	-
0.6CuMgAl	260	0.8	32.7	23.6	4.172	MgO	-	-	-	-	532	-
1.8CuMgAl	225	2.0	32.2	23.2	4.167	MgO	16.0	1.9	3.2^h	658	497	0.73
4.1CuMgAl	230	4.2	31.4	22.6	4.171	MgO	16.9	4.5	6.1	586	413	0.68
6.1CuMgAl	211	6.0	30.6	22.1	4.161	MgO	13.6	5.3	7.7	579	460	0.55
8.0CuMgAl	248	10.0	29.0	20.9	4.150	MgO	12.2	6.3	8.5	571	457	0.69
15.1CuMgAl	208	15.0	26.9	19.3	4.145	MgO + CuO	10.2	9.9	10.2	539	412	0.51
32.7CuMgAl	90	35.0	18.6	13.3	4.145	MgO + CuO	5.6	11.7	18.6	506	225	0.50
61.2CuMgAl	42	70.0	4.1	2.9	-	CuO	4.4	17.2	23.8	493	66	0.43
9.8CuMg	198	10.0	53.1	-	4.251	MgO	2.7	1.7	12.4^h	517	652	0.48
6.4CuAl	211	7.1	-	48.2	-	γ-alumina	13.9	5.7	7.5	518	45	0.68
MgO	192	-	60.3	-	4.216	MgO	-	-	-	-	655	-
Al$_2$O$_3$	230	-	-	52.9	-	γ-alumina	-	-	-	-	19	-

^{a} MgO lattice constant; ^{b} Cu^0 dispersion by N$_2$O decomposition; ^{c} exposed Cu^0 surface area; ^{d} Cu^0 particle size; ^{e} temperature at peak maximum by TPR; ^{f} base site number by TPD of CO$_2$; ^{g} mol 1,3-BDO/s mol surface Cu^0; ^{h} corrected using sample degree of reduction (see section **2.2**)
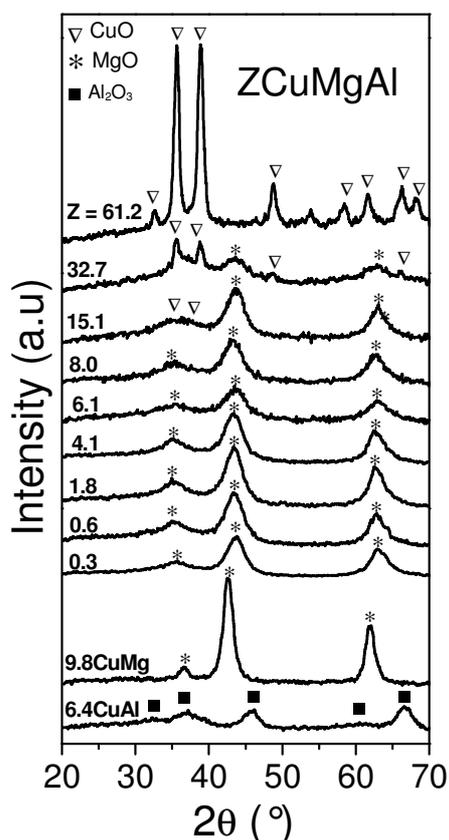
Figure 1: XRD patterns of ZCuMgAl, 9.8CuMg and 6.4CuAl catalysts.

Figure 2: TPR profiles of ZCuMgAl, 9.8CuMg and 6.4CuAl catalysts, and CuO as reference.

The fact that no copper species were detected at low Z values indicates that these species are either highly dispersed as small CuO crystallites not detectable by XRD or they are forming a solid solution within the oxide lattice. Similar effects were reported

by Xu et al. for CuMgCe oxides of up to 8 wt.% Cu[35] and by Tansoi et al. for CuMgAl oxides of comparable compositions.[36] An incipient CuO (tenorite, ASTM 5-0661) was observed at Z = 15.1 wt.%, Figure 1, this phase being clearly evident at higher Z values so

that it becomes the main crystalline species in sample 61.2CuMgAl. From the diffractograms of Figure 1, CuO crystallite sizes of 7.1 and 10.4 nm were calculated by the Scherrer´s equation for samples
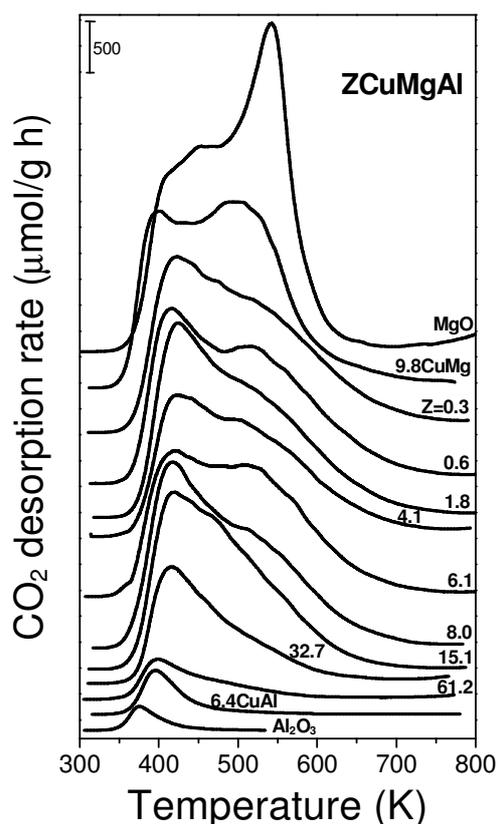
Figure 3: TPD of CO_2 on ZCuMgAl, 9.8CuMg, 6.4CuAl, MgO and Al_2O_3 catalysts.

32.7CuMgAl and 61.2CuMgAl, respectively.

      The reducibility of Cu species in ZCuMgAl samples was investigated by TPR. Figure 2 shows the reduction profiles obtained for ZCuMgAl samples calcined at 773 K; CuO, 9.8CuMg and 6.4CuAl were also included. Quantification of the reduced copper species considering that the observed peaks of Figure 2 correspond to $Cu^{2+} \rightarrow Cu^0$ reduction,[37] was carried out by previous calibration with pure CuO. The TPR of the 6.4CuAl sample showed stoichiometric reduction in a broad peak with a temperature at peak maximum (T_M) of 518 K, very close to that of pure CuO. Contrarily, in sample 9.8CuMg just 33% of the total copper atoms were reduced below 623 K and complete reduction was reached at 1100 K. It seems that for Cu-Al and Cu-Mg mixed oxides with 6-10wt.% Cu, whereas the Al^{3+} cations facilitate reduction of copper species as CuO, Mg^{2+} cations promote formation of a Cu-Mg solid solution in which Cu species are more difficult to reduce. As a result, the Cu^0 dispersion in sample 9.8CuMg (2.7%, Table 1) was much lower than in 6.4CuAl (13.9%).

      The ZCuMgAl samples reduced giving a single and broad reduction peak at around 450-650 K. Quantitative TPR analysis indicated that in the wide compositional range of 4.1-61.2wt.%, total reduction took place below 623 K . Contrarily, for samples with lower copper loadings (Z ≤ 1.8wt%), reduction was not complete and just less than 30% of the total copper atoms were reduced at that temperature.

      The temperature at the peak maximum (T_M) shifted to lower values as the Cu loading increases, gradually approaching that of the

reference bulk CuO, therefore suggesting the segregation of CuO species. The higher T_M values for low metal loading catalysts (Z≤1.8wt.%) is explained by a strong Cu-mixed oxide interaction probably because of formation at low Cu loadings of hardly reducible amorphous Cu-Mg or Cu-Al phases not detectable by XRD.[33,38] In addition, formation of a Cu-Mg solid solution that contributes to the low reducibility of ZCuMgAl samples with Z≤1.8wt.%, can be inferred from the calculations of their MgO lattice parameter (a_{MgO}), Table 1. Since the ionic radius of octahedrally coordinated Cu^{2+} ($r_{Cu2+} = 0.73$Å) is slightly larger than that of Mg^{2+} in MgO ($r_{Mg2+} = 0.72$Å),[39] the small expansion of the MgO lattice (higher a_{MgO} values) at low Cu loadings is the result of substitution of small amounts of Cu^{2+} for Mg^{2+} ions within the periclase structure, as postulated for sample 9.8CuMg. Solubility of the Cu^{2+} ions within the MgO structure is favored by the slight difference in ionic size between Cu^{2+} and Mg^{2+}.[34]

      Copper dispersion was calculated by combining TPR and N_2O chemisorption experiments in a two-step procedure as described in section **2.2.** Cu^0 dispersions (*D*), Table 1, between 4 and 17% were obtained for ZCuMgAl samples with copper loadings Z ≥ 1.8 wt.%. Below that copper content, meaningful dispersions could not be measured because of experimental limitations to operate under conditions free of artifacts.[25] Reduction temperatures above the oxide calcination temperature (773 K) would have been required to achieve complete sample reduction, with the consequent Cu^0 particle sintering.

      The *D* values monotonically decreased with increasing the Cu content revealing formation of larger Cu^0 particles (*L* values in Table 1), in agreement with the CuO crystallite size increase determined by XRD. However, the Cu^0 species surface area (A_{Cu}) gradually increased at higher loadings due to the fact that the drop of dispersion is overcompensated by the higher Z values (see section **2.2** for calculations). Thus, at high Z values the sample surface contains more Cu^0 particles of larger size.

      The surface basic properties of the ZCuMgAl, 9.8CuMg and 6.4CuAl samples were investigated by TPD of CO_2, Figure 3. By integration of the TPD curves, the number of base sites was calculated and results are shown in Table 1. Pure MgO desorbs CO_2 in a wide temperature range of 350-700 K, with a temperature at peak maximum of 540 K. Thus, the shape of the desorption curve for sample 9.8CuMg showing a peak maximum at ~500 K suggests that partial incorporation of copper in the MgO matrix causes the loss of strong base sites. However, the Cu-Mg mixed oxide retains the total number of base sites (652 µmol/g) of pure MgO (655 µmol/g). On the other hand, sample 6.4CuAl, that lacks of Mg^{2+} cations, desorbs CO_2 at lower temperatures (~400 K) and presents basic features comparable to those of Al_2O_3.

      Similarly to sample 9.8CuMg, the ZCuMgAl samples desorb CO_2 in the wide temperature range of 350-700 K, reflecting the presence of surface sites that adsorb CO_2 with different binding energies. However, the presence of acidic Al^{3+} cations in their formulation shifts the peak maximum to lower temperatures (~420 K) compared to 9.8CuMg. The shape of the TPD curves, that reflects the base strength distribution, is similar for all the ZCuMgAl samples but shows the gradual disappearance of the shoulder at ~520 K and the decrease of the total number of base sites as the copper content (Z) increases, Table 1. The latter is the consequence of the decreased Mg content, Table 1. Thus, the ZCuMgAl samples present basic properties, in terms of number and strength distribution, which are halfway between 6.4CuAl and 9.8CuMg.

3.2 Reaction pathways for 1,3-BDO conversion on bifunctional copper-based catalysts

      As depicted in Scheme 1, 1,3-BDO can undergo several

reactions forming numerous products. Recently,[21] we investigated the performance of a series of single oxides with Lewis acid properties for 1,3-BDO conversion in the gas phase. There, we classified the products in two major groups arising from initial dehydration or dehydrogenation reactions, Scheme 1; consecutive dehydration, hydrogenation and C-C bond cleavage reactions are also expected giving rise to several groups of compounds. Thus, the initial dehydration of 1,3-BDO leads to unsaturated alcohols (group UOL) such as 3-buten-2-ol (2-C_4UOL) and 2-buten-1-ol (1-C_4UOL), which can be converted consecutively via hydrogenation or dehydration reactions, into saturated alcohols (group SOL) or olefins (BD), respectively. Thus, the dehydration activity is defined as UOL, SOL and BD formation rates ($r_{-H2O} = r_{UOL} + r_{SOL} + r_{BD}$). Similarly, 1,3-BDO is initially dehydrogenated to hydroxycarbonyl compounds (group HY) such as 4-hydroxy-2-butanone (HYK) and 3-hydroxybutanal (HYAL). Only HYK was detected in significant amounts, thereby confirming the preferential dehydrogenation of the secondary OH function of 1,3-BDO. However, formation of small amounts of HYAL was inferred from consecutive products (C_2AL and C_2OL, Scheme 1). Both HY compounds can be further transformed to C_4 unsaturated and saturated ketones (group K) by dehydration-hydrogenation reactions or to C_1-C_3 oxygenates like alcohols, aldehydes and ketones (group RA) by retro-aldol-like reactions. Therefore, dehydrogenation activity comprises formation of HY, RA and K compounds ($r_{-H2} = r_{HY} + r_K + r_{RA}$). Thus, selectivities to dehydration and dehydrogenation products are defined as $S_{-H2O} = r_{-H2O}/r_{BDO}$ and $S_{-H2} = r_{-H2}/r_{BDO}$, respectively, where
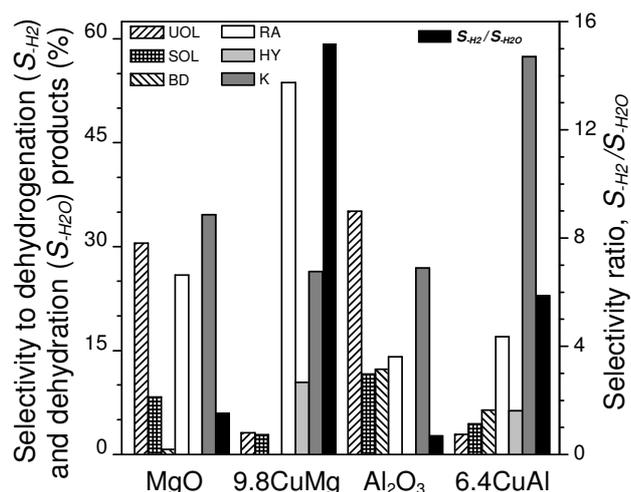
Figure 4: Selectivity ($S_i = r_i/r_{BDO}$) to dehydrogenation (i=K, RA and HY) and dehydration (i=UOL, SOL and BD) products and dehydrogenation/dehydration selectivity ratio (S_{-H2}/S_{-H2O}) on MgO, 9.8CuMg, Al_2O_3 and 6.4CuAl catalysts [T = 523K; $\bar{P}_{BDO}$ = 2.33kPa; X_{BDO} = 30%]

r_{BDO} stands for the overall 1,3-BDO conversion rate in mmol/h g cat.

MgO and Al_2O_3 are typical Lewis oxides with known acid-base properties,[29] Table 1. These reference materials were tested at 523K and 101.3 kPa. Figure 4 shows the selectivity ($S_i = r_i/r_{BDO}$) of these materials toward main dehydrogenation (HY, K and RA) and dehydration (UOL, SOL and BD) products, as well as the ratio between the selectivity toward dehydrogenation and dehydration products (S_{-H2}/S_{-H2O}) at 30% conversion. As can be observed, the main reaction pathway that takes place on a strongly basic catalyst such as MgO is 1,3-BDO dehydrogenation, the rest being dehydration products (S_{-H2}/S_{-H2O} = 1.5). On the contrary, on moderately acidic oxides such as Al_2O_3, the dehydration route

predominates over dehydrogenation (S_{-H2}/S_{-H2O} = 0.7).

Valuable unsaturated oxygenates such as alcohols (group UOL) and ketones (C_4UK in group K) are the main products on MgO and Al_2O_3. Contrarily, hydroxycarbonyl compounds (group HY, Scheme 1), the primary products of the dehydrogenation pathway, cannot be obtained in measurable amounts on these materials because they are rapidly converted on surface acid or base sites into products of groups K (mainly C_4UK) or RA by consecutive dehydration or C-C bond cleavage reactions, respectively.

On the other hand, in a previous work[20] on monofunctional metal catalysts such as Cu/SiO_2, we found that 1,3-BDO is dehydrogenated to HY compounds or converted to the saturated ketone C_4SK depending on the metal dispersion, whereas unsaturated oxygenates cannot be obtained in significant concentrations regardless of the Cu^0 dispersion values. Now, to elucidate the participation of copper species in bifunctional catalysts during the 1,3-BDO conversion, the reference samples 9.8CuMg and 6.4CuAl were tested. The effect of introducing a metal site into the formulation of acid or base single oxides is evident in the r_{BDO} values of the 9.8CuMg (71.9 mmol/g h) and 6.4CuAl (345.1 mmol/g h) catalysts that are 10 times higher than those of the corresponding single oxides, MgO (7.2 mmol/g h) and Al_2O_3 (30.7 mmol/g h). The presence of reducible copper species (Figure 2) in Cu-Al or Cu-Mg catalysts enhances the catalytic activity. This effect is interpreted in terms of the ability of the Cu^0 atoms to promote the O-H bond cleavage of 1,3-BDO at high rates, leading to a remarkable shift of the reaction pathway toward dehydrogenation reactions ($S_{-H2} \geq 80\%$, Figure 4), regardless of the acid or base nature of the mixed oxide.

Small amounts of surface Cu^0 species such as those on 9.8CuMg (A_{Cu} = 1.7 m^2/g, Table 1) are enough to form measurable amounts of HY compounds (10% selectivity to HY, Figure 4). Moreover, Cu^0 species readily promote hydrogenation steps such as that of the C=C bond of unsaturated oxygenates and therefore, unsaturated compounds are obtained in low concentrations (3% selectivity to UOL and 6% to C_4UK) on this catalyst. Even smaller selectivities toward these compounds were found on 6.4CuAl, Figure 4. In fact, the main product on 6.4CuAl is the less valuable saturated ketone (54% selectivity to C_4SK) probably formed not only by hydrogenation of C=C bonds but also by fast isomerization of UOL on metallic or acidic sites as postulated for Cu/SiO_2 catalysts,[20] Scheme 1.

Although the dehydrogenation route promoted by Cu^0 species predominates on both Cu-Mg and Cu-Al catalysts, participation of the acid or base site in the reaction pathways leading to different products cannot be excluded as indicated by the dehydrogenation/dehydration selectivity ratio; a much higher value was calculated on the strongly basic 9.8CuMg (S_{-H2}/S_{-H2O} =15.2) sample compared to the weakly basic 6.4CuAl (S_{-H2}/S_{-H2O} =5.9). Thus, from the selectivity point of view, the role of Cu^0 is to enhance the dehydrogenating properties of MgO in 9.8CuMg and to worsen the dehydrating performance of alumina in 6.4CuAl, Figure 4. These results confirm the metal-base or metal-acid bifunctional performance of Cu-Mg or Cu-Al catalysts.

3.3 Structure-activity relationship for ZCuMgAl catalysts

The catalytic performance of the ZCuMgAl samples of Table 1 was investigated at 523K and 101.3 kPa. The model diol molecule is converted on these catalysts through the complex reaction network of Scheme 1. Activity and selectivity of these materials depend on the copper content and therefore were quite different from the Cu-Mg or Cu-Al mixed oxides, or to the previously reported Cu/SiO_2 [20] and acid-base single oxides.[21]

The activity (r_{BDO}) and selectivity ratio (S_{-H2}/S_{-H2O}) values obtained on the ZCuMgAl catalysts are plotted in Figure 5. Figure 5
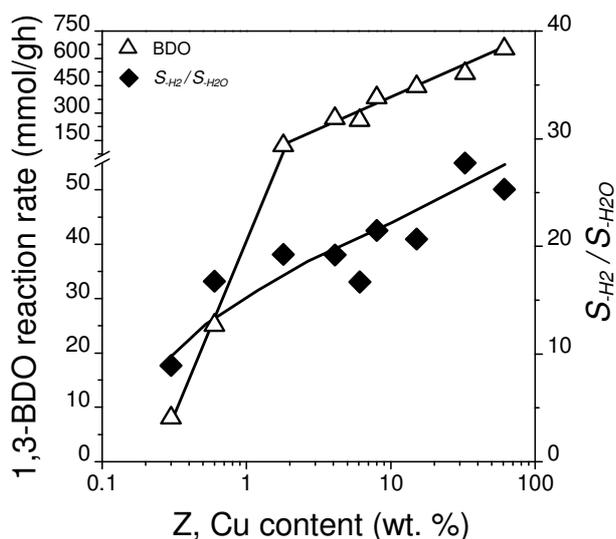
Figure 5: 1,3-BDO conversion rate (r_{BDO}) and dehydrogenation/dehydration selectivity ratio (S_{-H2}/S_{-H2O}) at 30% X_{BDO} on ZCuMgAl catalysts as a function of the copper content (Z) [T = 523K; $\bar{P}_{BDO}$ = 2.33kPa]

shows that r_{BDO} gradually increases with increasing the copper content (Z) from 0.3 to 61.2wt.%. Therefore, the lowest 1,3-BDO conversion rate was calculated for sample 0.3CuMgAl (r_{BDO} = 8.0 mmol/h g cat), a value similar to that of the pure MgO reference sample (r_{BDO} = 7.2 mmol/h g cat). The activity remains low for Z ≤1 wt.%; this result is accounted for the low content of reducible copper species in those samples, which hampered the Cu^0 dispersion measurement. On the other hand, a r_{BDO} value ~100 times larger was measured on 61.2CuMgAl.

The shape of the r_{BDO} curve differs from the one previously reported for Cu/SiO₂ catalysts showing a maximum value at Z~12wt.%, the loading corresponding to the silica exchange capacity.[20] This difference is attributed to the better properties of Mg-Al oxides to disperse Cu^0 particles compared to silica. For instance, on a 15wt% Cu/SiO₂ sample the Cu^0 dispersion

dramatically decreased to 7.8% compared to 25.3% measured for the 12wt.% sample showing the maximum r_{BDO} rate.

Using the catalytic results for 1,3-BDO conversion reactions, the dispersion of Cu^0 species estimated by TPR-N₂O decomposition and the number of surface base sites determined by TPD of CO₂, we can discuss now the effects of Cu metal particle size and oxide acid-base properties on r_{BDO}, the turnover rate (TOR) and selectivity.

We demonstrated earlier that surface Cu^{n+} species are inactive to promote neither the 1,3-BDO conversion nor the consecutive decomposition of HY compounds.[20] Here, we found that on ZCuMgAl catalysts the activity (r_{BDO}) increases linearly with the Cu^0 surface area (A_{Cu}, Table 1) as shown in the Supplementary Information. Thus, the TOR values measured for all the ZCuMgAl, 9.8CuMg and 6.4CuAl catalysts, Table 1, were similar, thereby confirming participation of reduced copper species in kinetically relevant reaction steps. Besides, particles sizes of these catalysts range from 3 to 25 nm showing that the Cu-catalyzed activation of the bonds participating in rate limiting steps is rather structure-insensitive, as previously reported for other alcohol dehydrogenation reactions.[40,41,42] In fact, we reported similar findings for the diol conversion on Cu/SiO₂ catalysts having a wide range of particle sizes.[20] Constant TOR values of ~1.2 s⁻¹ were obtained on Cu/SiO₂ catalysts having different copper contents and no measurable amounts of acid or base sites.

The high S_{-H2}/S_{-H2O} ratio, Figure 5, indicates that the ZCuMgAl catalysts mainly promote the 1,3-BDO dehydrogenation route. The r_{-H2} values are up to 100 times higher than on MgO and up to an order of magnitude higher than on 9.8CuMg. Contrarily, the dehydration performance of the ZCuMgAl catalysts is slightly worse than that of 6.4CuAl, in agreement with their stronger basic properties shown in Table 1 and Figure 3. The S_{-H2}/S_{-H2O} ratio measured at 30% conversion gradually increased with increasing Z from 9 for 0.3CuMgAl to 26 for 61.2CuMgAl. Thus, the catalyst dehydrogenating properties are enhanced at high loadings where the amount of exposed Cu^0 species is higher (Table 1).

The distribution of dehydrogenation (r_i/r_{-H2}; i = K, HY and RA) and dehydration (r_i/r_{-H2O}; i = UOL, SOL and BD) products also depends on the metal loading as presented in Figure 6. Figure 6A suggests that the primary products of dehydrogenation reactions (HY compounds, Scheme 1) cannot be obtained in significant amounts on
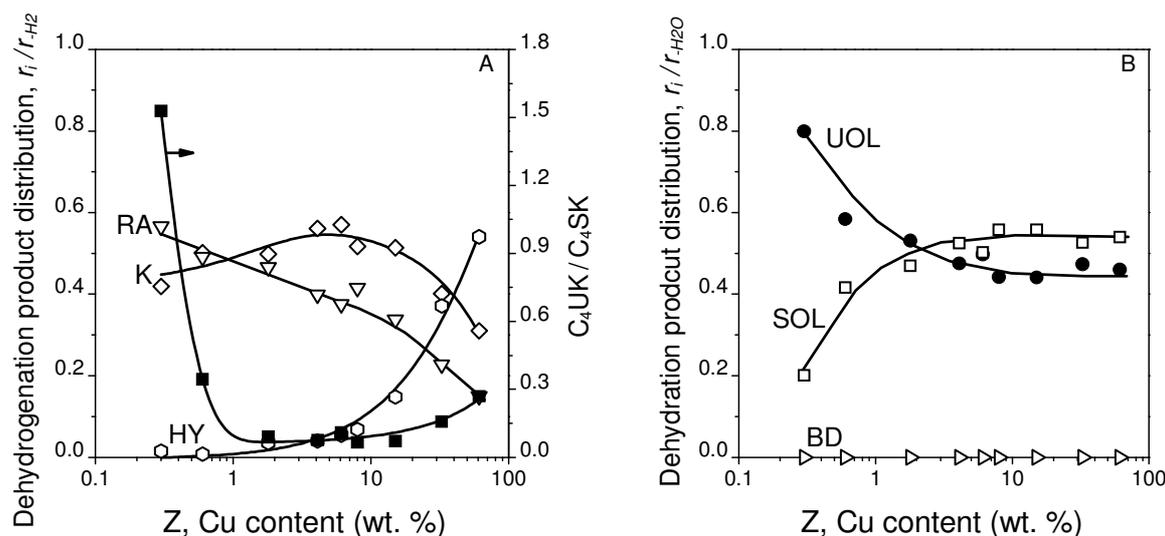
Figure 6: Product distribution on ZCuMgAl catalysts as a function of the copper content (Z). (A) Dehydrogenation (r_i/r_{-H2}; i = K, RA and HY); (B) Dehydration (r_i/r_{-H2O}; i = UOL, SOL and BD) [T = 523K; $\bar{P}_{BDO}$ = 2.33kPa; X_{BDO} = 30%]

low copper loading ZCuMgAl catalysts. As explained above, compounds of group HY are unstable under gas-phase reactions conditions and according to Figure 4, surface base sites such as those of MgO completely transform them in compounds of groups RA and K. Moreover, we recently investigated the role of the Cu^0 particle size on the selectivity of Cu/SiO_2 catalysts for 1,3-BDO conversion.[20] We demonstrated there that the selectivity can be oriented toward HY compounds (mainly the hydroxyketone HYK) by using catalysts with large Cu^0 particles. On such particles, the HYK-Cu^0 site interaction is weak and therefore, the HYK molecule is released to the gas phase before being converted in consecutive reactions.

In line with the results on acid-base single oxides and on Cu/SiO_2 catalysts, the lack of HY compounds among the distribution of dehydrogenation products on ZCuMgAl catalysts with low Z values, Figure 6A, is explained by the fact that those catalysts contain the largest number of base sites and the smallest Cu^0 particle sizes. Nevertheless, the contribution of group HY increases with Z and predominates on sample 61.2CuMgAl ($r_{HYK}/r_{-H2} = 0.54$) because of a combination of large Cu^0 particles and low number of base sites in this catalyst. Furthermore, at low Z values the strong adsorption of HY compounds on the enhanced number of exposed basic sites favors not only the consecutive transformation of HY into the ketones of group K, but also the base-catalyzed retro-aldolization reactions giving C_1-C_3 oxygenates (group RA). Contrarily, on high copper content ZCuMgAl catalysts, the low basicity of these materials (Table 1 and Figure 3) accounts for the small contribution of group RA.

The distribution of dehydration products on ZCuMgAl catalyst is presented in Figure 6B. As explained above, ZCuMgAl catalysts mainly promote the initial dehydrogenation of 1,3-BDO giving S_{-H2O} values of less than 10% at 30% conversion. Formation of the primary products of the dehydration pathway, the unsaturated alcohols (UOL), is favored at low Z values. At higher copper contents, the consecutive hydrogenation of the C=C bond of UOL toward saturated alcohols (SOL) takes place as a result of the increasing catalyst dehydrogenating properties (high S_{-H2}/S_{-H2O}, Figure 5) arising from the higher A_{Cu}. None of the ZCuMgAl catalysts dehydrates UOL to butadiene (BD).

Regarding hydrogenation of unsaturated bonds, it is worth mentioning that since the reactions are carried out in an inert atmosphere, the only surface hydrogen fragments available for reduction of C=C or C=O bonds (Scheme 1) are those generated by 1,3-BDO initial dehydrogenation. Thus, at low Z values, where A_{Cu} and S_{-H2}/S_{-H2O} are the lowest, the catalyst surface is deprived of hydrogen and therefore unsaturated oxygenates prevail as shown in Figure 6B for unsaturated and saturated C_4 alcohols. Figure 6A shows that effect for the unsaturated (C_4UK) and saturated (C_4SK) ketones of group K.

3.4 Formation of multifunctional oxygenates on ZCuMgAl catalysts

The previous findings on acid-base single oxides and on Cu/SiO_2 catalysts suggested that it is not possible to simultaneously produce on those materials all the different multifunctional oxygenates at high rates, i.e., compounds that combine different chemical functions such as C=O and OH (group HY) or C=C and C=O (C_4UK in group K) or C=C and OH (group UOL).

We showed in Figure 4 that catalyst 9.8CuMg presents a slightly better selectivity of 19% toward those valuable compounds (HY+C_4UK+UOL) compared to the 12% on sample 6.4CuAl, but the activity of the former is much lower than that of the latter. Nevertheless, the Cu-Mg-Al elemental combination in ZCuMgAl catalysts, gives rise to basic properties that are in between of those of

9.8CuMg and 6.4CuAl and proved to be suitable for formation of multifunctional chemical compounds with selectivities of up to ~60% at moderate reaction rates. Figure 7 shows that by properly choosing the Cu loading it is possible to tune the distribution of multifunctional compounds due to the fact that the reactant and product interaction with the surface sites (basic or metallic) determines the selectivity pattern. Unsaturated oxygenates such as the ketone (C_4UK) and to a lesser extent, the unsaturated alcohols
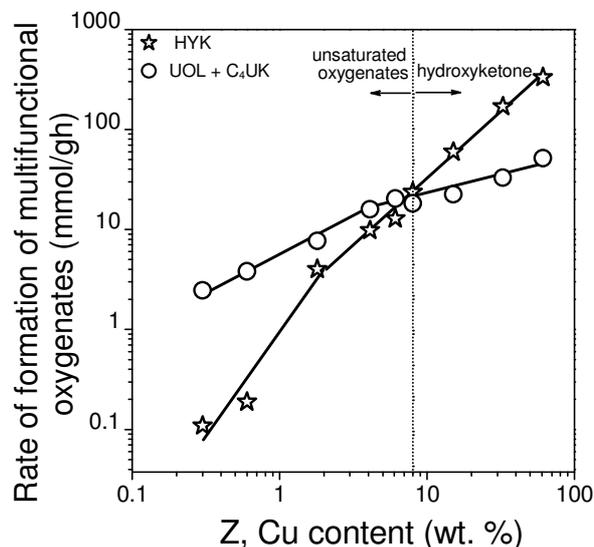
Figure 7: Rate of formation of multifunctional oxygenates (unsaturated oxygenates: UOL + C_4UK; hydroxyketone: HYK) on ZCuMgAl catalysts as a function of the copper content (Z) [$T = 523K$; $\bar{P}_{BDO} = 2.33kPa$]
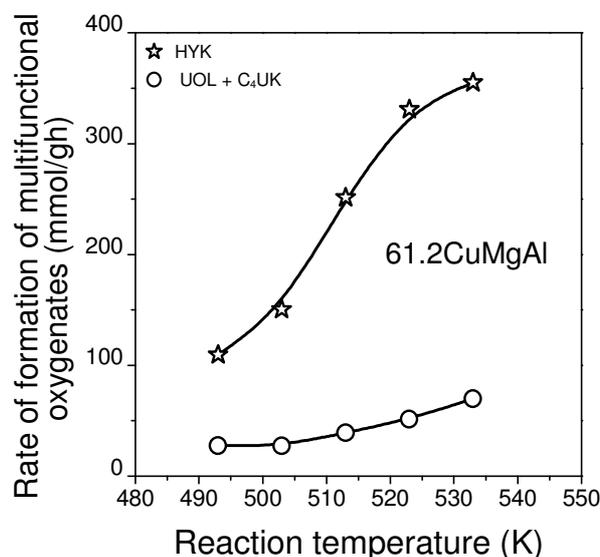
Figure 8: Rate of formation of multifunctional oxygenates (unsaturated oxygenates: UOL + C_4UK; hydroxyketone: HYK) on 61.2CuMgAl as a function of the reaction temperature [$\bar{P}_{BDO} = 2.33kPa$]

(UOL) can be obtained at Z≤8wt.% because the dehydration reactions steps involved in UOL and C_4UK formation (Scheme 1) are promoted on surface base sites or small Cu^0 particles. On the other hand, the release to the gas phase of the hydroxyketone formed

by 1,3-BDO dehydrogenation is favored on larger Cu^0 particles such as those present at high copper contents (catalysts with Z > 8wt.%).

From the results of Figure 7, sample 61.2CuMgAl was chosen to investigate the effect of the reaction temperature on the rate of formation of multifunctional oxygenates. The selectivities toward multifunctional compounds are just slightly modified (55-63%) by changing the temperature, which is typical of complex reaction networks involving consecutive or parallel reaction steps. However, Figure 8 shows that the rate of formation of both, the hydroxyketone (HYK) and the unsaturated oxygenates $(UOL+C_4UK)$, can be improved at increasing temperatures. A more marked effect of temperature is observed on the hydroxyketone curve, this result being explained by the higher apparent activation energy calculated for HYK (16.4 kcal/mol) compared to that for unsaturated oxygenates (13.0 kcal/mol).

4. Conclusions

Polyols resulting from bio-resources can be upgraded to valuable oxygenates by a combination of dehydration and dehydrogenation reactions in the gas phase. In particular, the model molecule, 1,3-butanediol, can be transformed on bifunctional Cu-Mg-Al mixed oxide catalysts. These materials were prepared with different copper contents and Mg/Al =1.5 (molar ratio) so that to ensure mild acid-base properties and a proper dispersion of the metallic phase.

Previous findings indicate that acid-base single oxides give unsaturated alcohols and ketones by dehydration reactions at low rates. They also completely transform the initial 1,3-butanediol dehydrogenation product, a hydroxyketone (4-hydroxy-2-butanone) into other products by consecutive reactions. On the other hand, metallic catalysts such as Cu/SiO_2 transform 1,3-butanediol at high rates but production of multifunctional compounds is limited to just the hydroxyketone formed selectively on large Cu^0 particles. In contrast, the bifunctional Cu-Mg-Al catalysts studied here convert 1,3-butanediol at rates that are in between of those of acid-base single oxides and silica-supported Cu^0 catalysts. Besides, on Cu-Mg-Al catalysts the diol reaction rate is strongly dependent on the copper content so that the catalyst activity increases linearly with the amount of exposed Cu^0 sites. Thus, catalysts with high copper loadings are more active because they contain a larger number of surface Cu^0 sites.

Metallic copper sites promote mainly the initial reactant dehydrogenation whereas the initial dehydration reaction occurs at much lower rates regardless of the copper content. Thus, the dehydrogenation/dehydration selectivity ratio is enhanced at high metal loadings where Cu^0 sites are more abundant.

Low copper content Cu-Mg-Al catalysts yield multifunctional oxygenates at low rates. Catalysts with copper content above 8 wt.% are more interesting materials because they form the hydroxyketone at much higher rates giving simultaneously but, to a lesser extent, unsaturated oxygenates.

The distribution of dehydrogenation and dehydration products depends not only on the amount of Cu^0 sites but also on the acid-base properties of the oxide matrix. Therefore, in addition to being less active, low copper content catalysts, with a large number of surface base sites, give C_1-C_3 oxygenates by C-C bond cleavage reactions. Similar catalytic behavior is found on a strongly basic Cu-Mg oxide. More acidic oxides such as Cu-Al convert the diol into the saturated ketone and olefins. Thus, an adequate balance between basic and metallic sites is needed to attain reasonable activity and selectivities toward industrially attractive oxygenates.

Acknowledgements

References

1 *"Top Value Added Chemicals From Biomass",* T. Werpy, G. Petersen, Eds., US DOE Report, 2004.
2 A. Corma, S. Iborra, and A. Velty, *Chem. Rev.*, 2007, **107,** 2411-2502.
3 A. Corma, G.W. Huber, L. Sauvanaud and P. O'Connor, *J. Catal.*, 2007, **247**, 307-327.
4 R.D. Cortright, R.R. Davda and J.A. Dumesic, *Nature*, 2002, **418**, 964-967.
5 Y. Liu, H. Tuysuz, C.-J. Jia, M. Schwickardi, R. Rinaldi, A-H. Lu, W. Schmidt and F. Schuth, *Chem. Commun.*, 2010, **46**, 1238-1240.
6 N. Ichikawa, S. Sato, R. Takahashi and T. Sodesawa, *J. Molec. Catal. A: Chem.*, 2006, **256**, 106-112
7 N. Ichikawa, S. Sato, R. Takahashi, T. Sodesawa and K. Inui, *J. Molec. Catal. A: Chem.*, 2004, **212**, 197-203.
8 S. Sato, M. Akiyama, R. Takahashi, T. Hara, K. Inui and M. Yokota, *Appl. Catal. A: General*, 2008, **347**, 186-191.
9 C.W. Chiu, M.A. Dasari and G.J. Suppes, *AIChE J.*, 2006, **52(10)**, 3543-3548.
10 S. Sato, R. Takahashi, T. Sodesawa, H. Fukuda, T. Sekine and E. Tsukuda, *Catal. Comm.,* 2005, **6**, 607-610.
11 S. Sato, R. Takahashi, H. Fukuda and K. Inui, *J. Molec. Catal. A: Chem.*, 2007, **272**, 164-168.
12 A. Corma, G. W. Huber, L. Sauvanaud and P. O'Connor, *J. Catal.*, 2008, **257**, 163-171.
13 Z-L. Xiu and A.-P. Zeng, *Appl. Microbiol. Biotechnol.*, 2008, **78**, 917-926.
14 N. Kazuhisa, *EP 0787709A1*, 1997, to Daicel Chemical Industries Ltd.
15 K.Windhorst and R.D. Guajardo, *WO 068408A1*, 2005, to Celanese International Corporation.
16 T. Mukaiyama, *Org. React.*, 1982, **28**, 203-331.
17 H. Zhang, G.T. Lountos, C.B. Ching and R. Jiang, *Appl. Microbiol. Biotechnol.*, 2010, **88**, 117-124.
18 Y. Su, Y.-M. Liu, L.-C. Wang, M. Chen, Y. Cao, W.-L. Dai, H.-Y. He and K.-N. Fan, *Appl. Catal. A: General*, 2006, **315**, 91-100.
19 N. Ichikawa, S, Sato, R. Takahashi and T. Sodesawa, *Catal. Comm.*, 2005, **6**, 19-22.
20 P.A. Torresi, V.K. Díez, P.J. Luggren and J.I. Di Cosimo, *App. Catal. A: General*, 2013, **458**, 119-129.
21 V.K. Díez, P.A. Torresi, P.J. Luggren, C.A. Ferretti and J.I. Di Cosimo, *Catal. Today*, 2013, **213**, 18-24.
22 P.L. Spath and D.C. Dayton, *National Renewable Energy Laboratory*, NREL/TP-510-34929, technical report, 2003.
23 J. I. Di Cosimo, G. Torres and C. R. Apesteguía, *J. Catal.*, 2002, **208**, 114-123.
24 J.I. Di Cosimo, V.K. Díez and C.R. Apesteguía, *Appl. Catal. A: General*, 1996, **13**, 149-166.
25 D. A. Monti and A. Baiker, *J. Catal.*, 1983, **83**, 323-335.
26 P. Malet and A. Caballero, *J. Chem. Soc., Faraday Tans. I*, 1988, **84**, 2369-2375.
27 E.D. Guerreiro, O.F. Gorriz, J.B. Rivarola and L.A. Arrúa, *Appl. Catal. A: General*, 1997, **165**, 259-271.
28 G. C. Bond and S.N. Namijo, *J. Catal.*, 1989, **118**, 507-510.
29 C.A. Ferretti, A. Soldano, C.R. Apesteguía and J.I. Di Cosimo, *Chem. Eng. J.*, 2010, **161**, 346-354
30 G. Torres, C.R. Apesteguía and J.I. Di Cosimo, *Appl. Catal. A: General*, 2007, **317**, 161-170.
31 J.I. Di Cosimo, A. Acosta and C.R. Apesteguía, *J. Molec. Catal. A: Chemical*, 2004, **222**, 87-96.
32 J. I. Di Cosimo, V. K. Díez, M. Xu, E. Iglesia and C. R. Apesteguía, *J. Catal.*, 1998, **78**, 499-510.
33 R.T. Figueiredo, H. Martins Carvalho Andrade and J.L.G. Fierro, *J. Molec. Catal. A: Chemical*, 2010, **318**, 15-20.
34 T. Sato, H. Fujita, T. Endo and M. Shimada, *React. of Solids*, 1988, **5**, 219-228.

35 M. Xu, M.J.L. Gines, A. Hilmen, B.L. Stephens and E. Iglesia, *J. Catal.*, 1997, **171**, 130-147.

36 S. Tanasoi, N. Tanchoux, A. Urda, D. Tichit, I. Sandulescu, F. Fajula, I.-C. Marcu, *Appl. Catal. A: General,* 2009, **363**, 135-142.

37 J.I. Di Cosimo and C.R. Apesteguía, *J. Molec. Catal.*, 1994, **91**, 369-386.

38 S. Gusi, F. Trifiró and A. Vaccari, *React. Solids*, 1986, **2(1-2)**, 59-71.

39 http://abulafia.mt.ic.ac.uk

40 M. J. L. Ginés and E. Iglesia, *J. Catal.*, 1998, **176**, 155-172.

41 F.-W. Chang, W.-Y. Kuo and K.-C. Lee, *Appl. Catal. A: General*, 2003, **246**, 253-264.

42 R.M. Rioux and M.A. Vannice, *J. Catal.*, 2003, **216**, 362-376.

Catalysis Science & Technology Accepted Manuscript